IMPROVING DELAMINATION STRENGTH THROUGH CNTS REINFORCEMENT: NUMERICAL SIMULATION

Y. EL ASSAMI[1], M. DRISSI HABTI[1*#], V. RAMAN[2] and A. PISUPATI[1]

[1]PRES LUNAM IFSTTAR, MACSI/COSYS
CS4 Route de Bouaye 44344 Bouguenais Cedex, France

[2]Institut de Recherche Technologique (IRT) Jules VERNE
Chemin du Chaffault, 44340 Bouguenais, France

Emails: yassine.el-assami@ifsttar.fr, monssef.drissi-habti@ifsttar.fr,
venkadesh.raman@irt-jules-verne.fr, anurag.pisupati@ifsttar.fr

[*]Director of Consortium DURSI (blog: http://macsisit.blogspot.fr/)
[#]To whom correspondences should be addressed

Keywords: Nanotubes, Composites, Polymer, Reinforcement, Homogenization

Abstract

In order to improve the resistance to delamination, a carbon nanotube (CNT) reinforced resin can be added, as a glue, to bond the layers, thus enhancing significantly the shear strength. The mechanical performance of the CNTs increases the resistance and the elastic moduli of the resin. In order to evaluate the enhanced mechanical properties following the addition of CNTs, a multiscale approach based on Finite Element Method (FEM) is carried-out. The proposed simulations will take into account parameters such as the volume fraction, the chirality and the orientation of CNTs. The mechanical properties deduced from this multiscale approach will allow determining the properties of a new bonding layer that would be considered in macroscopic models.

1. Introduction

The improvement of mechanical properties of polymers through the addition of Carbon nanotubes (CNTs) was studied recently using FEM analysis [1]–[5]. CNTs are known for their very high mechanical properties [6], [7]. Their tensile modulus is around 1 TPa (five times that of steel) and the covalent bonding between its atoms result in a high tensile strength (around 20 GPa [8]). Adding a small amount (weight fraction usually between 0.4% and 1%) of these nanotubes to a polymer matrix improves significantly its mechanical properties [9], [10].

In the present work, a FEM model of a CNT reinforced polymer is implemented. This model represents a first step study towards a multiscale approach to evaluate the properties of reinforced polymeric structures. It is worthwhile to note that the size of the CNTs that are industrially used is of a few tens of nanometers, the used FEM models are practical to handle nanotubes of these sizes and their interactions with the matrix (complex molecular structure).

Excerpt from ISBN 978-3-00-053387-7

CNTs are modelled using a molecular mechanics approach [11]–[13], which allows handling in the same simulation the CNT (defined at the atomic scale [14]–[16]), the polymer matrix (as a continuous medium) and the interface (as a continuous layer with the effective behavior of van der Waals forces [17], [18]).
The effect of the reinforcement on the elastic properties of a nano-composite will be evaluated. As we can expect, for a tensile (or compression) test, the reinforcement is optimal if the CNT is parallel to the load. However, the shear modulus at a macroscale may not be significantly improved in the domain of elasticity. An elastoplastic model is proposed to point out the benefit of adding the CNT in shear tests.

2. Homogenization Problem

To study the reinforcing effect of a CNT, a FEM model is established where the covalent bonds of the nanotubes are modeled by beam elements, the polymer as a continuous field and the interface as a continuous layer that has the cohesive effective properties of van der Waals forces.
CNT weight fraction of $f_w = 1\%$ is routinely reported in the bibliography [19]–[22] and will be considered for all following simulations. The matrix volume will depend on its density and the number of atoms in the CNT:

$$V_{\mathrm{mat}} = \left(\frac{1}{f_w} - 1\right)\frac{n_C M_C}{\rho_{\mathrm{mat}}} \tag{1}$$

where V_{mat} is the volume of the matrix in the RVE, n_C is the number of carbon atoms in the CNT, M_C is the mass of one carbon atom and ρ_{mat} is the density of the matrix.

2.1. Nanotubes

The CNTs are simulated by a finite element lattice, where the C–C covalent bonds are represented by cylindrical beams of length, L, and radius, r, so that:

$$\frac{EA}{L} = k_r \quad , \quad \frac{EI}{L} = k_\theta \quad , \quad \frac{GJ}{L} = k_\tau \tag{2}$$

E and G being the Young's and shear moduli of the beam, $A = \pi r^2$ its section area, $I = \frac{\pi r^4}{4}$ its second moment and $J = \frac{\pi r^4}{2}$ its polar moment. k_r, k_θ and k_τ are the bond force constants of stretching, bending and torsional resistance calculated from the potential functions of molecular mechanics [23].

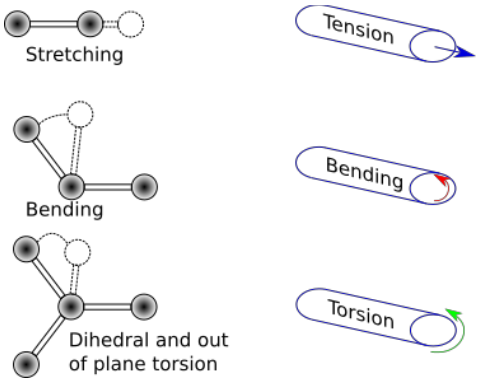

Figure 1. Analogy between atomic interactions and molecular mechanics.

Excerpt from ISBN 978-3-00-053387-7

The expression of these potentials is recalled in [6], [10], [12], [24]. These equations translate an analogy between the molecular interactions and the beam theory (Figure 1) [12], [13]. The properties of the representative circular beam are:

$$r = 4\sqrt{\frac{k_\theta}{k_r}} \quad , \quad E = \frac{k_r^2 L}{4\pi k_\theta} \quad , \quad G = \frac{k_r^2 k_\tau L}{8\pi k_\theta^2} \tag{3}$$

$\mathrm{L} = 0.1421$ nm is the length of the covalent bond C–C [23]. As for bond force constants, different values were assumed in the literature. A discussion was presented by Lu and Hu [16] about these parameters, which values can impact the results. The direct application of Equations (3) yield in some cases a Poisson's ratio greater than 0.5 [15], [25], [26]. In this paper, the approach of Lu and Hu [16] for choosing Poisson's ratio (based on the work of Scarpa and Adhikari [27]) will be adopted: $\mathrm{k_r} = 786$ nN/nm, $\mathrm{k_\theta} = 0.901$ nN nm/rad^2 and $\nu = 0.0344$. So, the Young's modulus of the beam elements is $\mathrm{E} = 7753$ GPa and the section radius is $\mathrm{r} = 0.0677$ nm.

Beam diameter is not necessarily related to the thickness of CNTs, as it is assumed in the approach of Scarpa and Adhikari [27]. To calculate the Young's modulus $\mathrm{E_{cnt}}$, we consider that the CNT has the same thickness of a graphene sheet, $\mathrm{t} = 0.34$ nm [13], [16]:

$$E_{\mathrm{cnt}} = \frac{F}{\pi\left(R_{\mathrm{cnt}} + \frac{t}{2}\right)^2 - \pi\left(R_{\mathrm{cnt}} - \frac{t}{2}\right)^2} \frac{L_{\mathrm{cnt}}}{\Delta L_{\mathrm{cnt}}} \tag{4}$$

F being the tensile force applied to a CNT and $\mathrm{\Delta L_{cnt}/L_{cnt}}$ the elastic strain of the nanotube. With the set of parameters presented above, a Young modulus $\mathrm{E_{cnt}}$ around 1.18 TPa is found.

2.2. Interface

CNT is assumed linked to the matrix only by van der Waals forces. These forces are accounted for by considering an average behavior of all interactions between a CNT and the matrix. Jiang and al. [17] calculated a cohesive behavior of the interface, based on the densities of interacting particles and the potential constants:

$$\sigma_{\mathrm{coh}} = 2\pi\rho_p\rho_c\varepsilon\sigma^2\left[\frac{\sigma^4}{(h+v)^4} - \frac{2\sigma^{10}}{5(h+v)^{10}}\right] \tag{5}$$

Equation (5) gives the relation between the tensile cohesive stress σ_{coh} and the opening v. It takes into account the volume density, ρ_p, of the polymer interacting atoms, the surface density of the CNT carbon atoms, ρ_c, and the Lennard–Jones 6–12 potential constants ε (bond energy at the equilibrium distance) and σ (related to the equilibrium distance between the atoms).

The equilibrium distance between the CNT and the polymer is $h = \left(\frac{2}{5}\right)^{\frac{1}{6}}\sigma$. It corresponds to the minimum potential from which the tensile stress is derived. Under the hypothesis of small strain, we can use the dominant parts of the Taylor expansion of σ_{coh}. The slope of the curve $\mathrm{h}\sigma_{\mathrm{coh}}$ around 0 corresponds to the Young's modulus of the interface layer:

$$E_{\mathrm{int}} = 30\left(\frac{2}{5}\right)^{\frac{1}{3}}\pi\rho_p\rho_c\varepsilon\sigma^2 \tag{6}$$

For our numerical applications, we adopt the same as those mentioned by Jiang and al. [17], $\sigma = 0.3825$ nm and $\varepsilon = 7.462 \times 10^{-4}$ nN · nm, $\rho_c = \frac{4}{3\sqrt{3}\mathrm{L}^2} = 38.1$ nm^{-2} and $\rho_p = 31.0$ nm^{-3}.

The cohesive law calculated for the shear depends on the sliding displacement, the opening and the length of the CNT. It does not vanish even though there is no sliding, but its value is much smaller

Excerpt from ISBN 978-3-00-053387-7

than the cohesive tensile stress. To account for the shear in the following simulations, a Poisson's ratio equal to that of the polymer is considered.

2.3. Polymer and RVE

The polymer is modeled as a continuous soft isotropic material. Its elastic properties are: $E_{mat} = 3.66\ nN/nm^2$, $\nu_{mat} = 0.358$ and the yield stress is $0.026\ nN/nm^2$ [28].

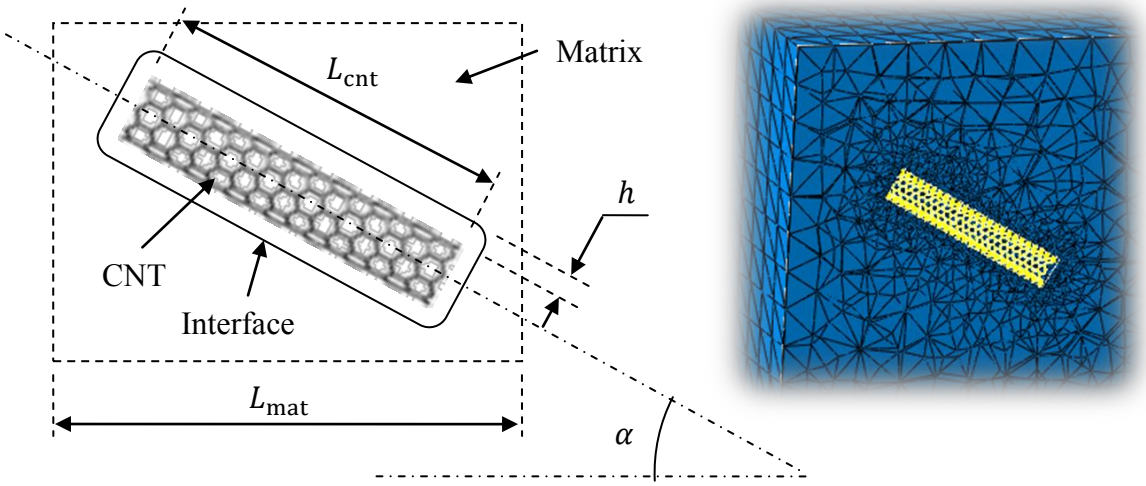

Figure 2. Geometry and an example of the mesh used in the finite element simulations.

For the following simulations, we consider that the CNT is completely embedded inside the matrix and that all the boundary conditions are applied on its outside border.

3. Results

3.1. Macroscopic stiffness of the reinforced polymer

In order to calculate the stiffness tensor of the reinforced epoxy, a FEM model of a cuboid RVE has been used (Figure 4.a). A displacement u, compatible with a macroscopic strain E, is imposed on the border of the RVE: $u = E.x$, where x is the coordinate of the points of the boundary. In order to obtain the macroscopic stiffness tensor, a tension ($E = e_i \otimes e_i, i \in \{1,2,3\}$) and a pure shear ($E = e_i \otimes^s e_j, i,j \in \{1,2,3\}, i \neq j$) are applied on the boundary.

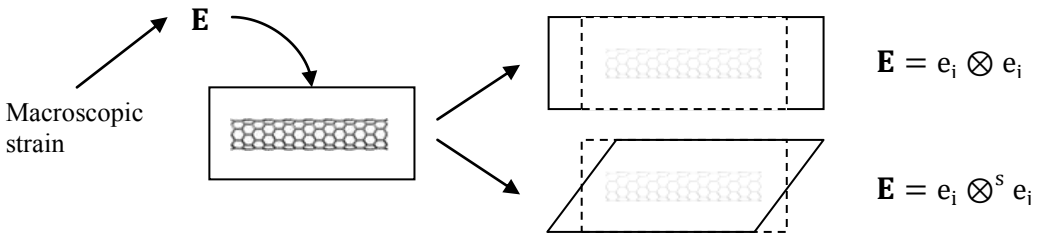

Figure 3. RVE used to calculate the stiffness tensor.

Excerpt from ISBN 978-3-00-053387-7

The macroscopic stiffness tensor $\mathbb{C}$ (the Voigt notation is used) is as follows:

$$\mathbb{C} = \begin{bmatrix} \frac{1}{E_1} & -\frac{\nu_{12}}{E_1} & -\frac{\nu_{13}}{E_1} & 0 & 0 & 0 \\ -\frac{\nu_{12}}{E_1} & \frac{1}{E_1} & -\frac{\nu_{13}}{E_1} & 0 & 0 & 0 \\ -\frac{\nu_{13}}{E_1} & -\frac{\nu_{13}}{E_1} & \frac{1}{E_3} & 0 & 0 & 0 \\ 0 & 0 & 0 & \frac{1}{2G_{13}} & 0 & 0 \\ 0 & 0 & 0 & 0 & \frac{1}{2G_{13}} & 0 \\ 0 & 0 & 0 & 0 & 0 & \frac{1+\nu_{12}}{E_1} \end{bmatrix}^{-1} = \begin{bmatrix} 6.15 & 3.43 & 3.41 & 0 & 0 & 0 \\ 3.43 & 6.15 & 3.41 & 0 & 0 & 0 \\ 3.41 & 3.41 & 10.47 & 0 & 0 & 0 \\ 0 & 0 & 0 & 2.73 & 0 & 0 \\ 0 & 0 & 0 & 0 & 2.73 & 0 \\ 0 & 0 & 0 & 0 & 0 & 2.73 \end{bmatrix} \quad (7)$$

The obtained stiffness corresponds to a transversely isotropic material (the volume average of the stress and strain fields is calculated from the boundary using the divergence theorem). The macroscopic elastic parameters of the composite are presented in the Table 1:

Table 1. Comparison of the elastic properties between the reinforced and pure polymer matrix.

	E_1 (GPa)	E_3 (GPa)	ν_{12}	ν_{13}	G_{13} (GPa)	G_{12} (GPa)
Nano-Composite	3.98	8.04	0.46	0.18	1.36	1.36
Net Polymer Matrix	3.66	3.66	0.36	0.36	1.35	1.35
% of Increase	1.09	2.19	-	-	1.01	1.01

As expected, the Young's modulus in the direction of the CNT is doubled with only 1% of weight fraction. However, shear properties remain close to those of the matrix.

3.2. Shear test

Figure 4 is emphasizing the way the shear calculations have been conducted. The bond layer is stiffened by CNTs and a single CNT that can be oriented from 0° to 90° is considered in a nano-cell that is loaded under shear (Figure 5).

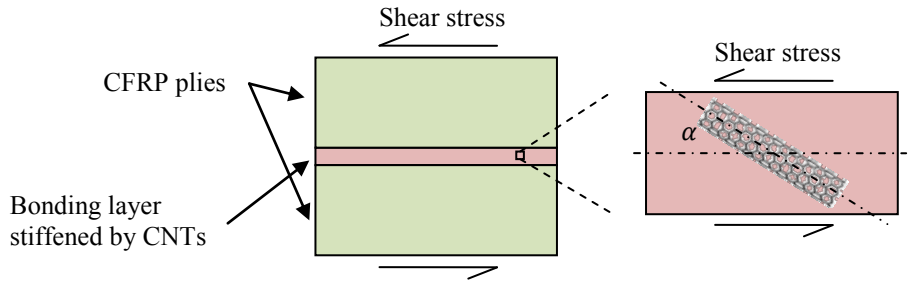

Figure 4. Schematic of bonding layer reinforced with CNTs experiencing shear stress.

Excerpt from ISBN 978-3-00-053387-7

In order to evaluate the effect of CNTs in the bonding layer, we consider a cuboidal domain of polymer containing a CNT, under a shear loading. Three parts are defined in this cuboid based on the boundary conditions: an upper and a lower domains of the same size, separated by a thin layer (which thickness is 10% the height of the domain). The upper and lower domains are considered as if they were inside infinitely rigid nano-grips. The lower part is fixed and a displacement is applied on the upper part, subjecting the middle region to shear stress (Figure 5).

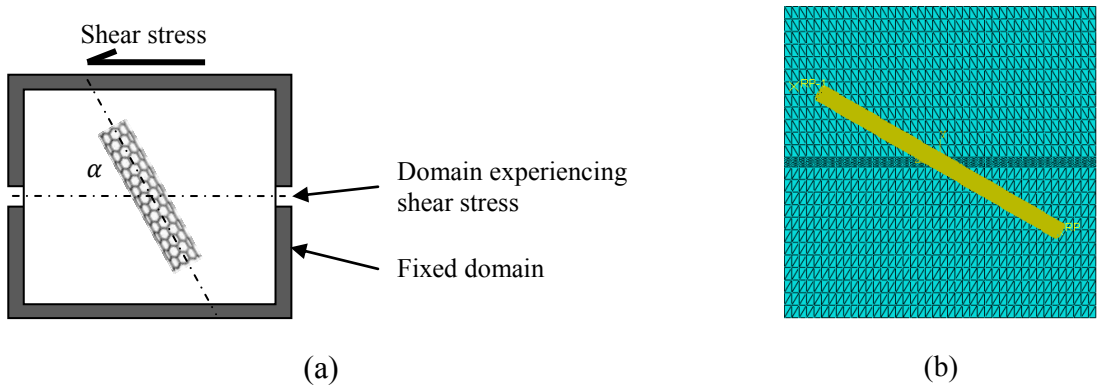

Figure 5. Shear experience: (a) Schematic of the boundary conditions. (b) Cross section of a mesh ($\alpha = 30°$).

An elastoplastic model is used to account for the nonlinear behavior of the matrix. The orientation of the CNT is controlled by the angle α (α = 0°: the CNT is parallel to the shear. α = 90°: the CNT is perpendicular to the shear plane).

Figure 6 shows the resultant force applied on the upper region of the block (normalized by the maximum force of the simulation without CNT) as a function of its displacement (normalized by the thickness of the area under shear). As known, the net polymer resin breaks in a brittle way. In other words, once the shear strength is reached, the net matrix will separate in 2 independent blocks. In the case of the RVE representing the bond joint reinforced by the CNT, once shear stress is applied, the effect of nano-reinforcement can be observed. Hence, the RVE will deform in a non-linear way. The simulations are plotted in Figure 6.a and 6.b, where a comparison has been made between the cases of the net resin (its shear strength is considered when the region experiencing shear reaches the yield stress) versus the nano-reinforced resin with the CNT that was oriented at various values of α.

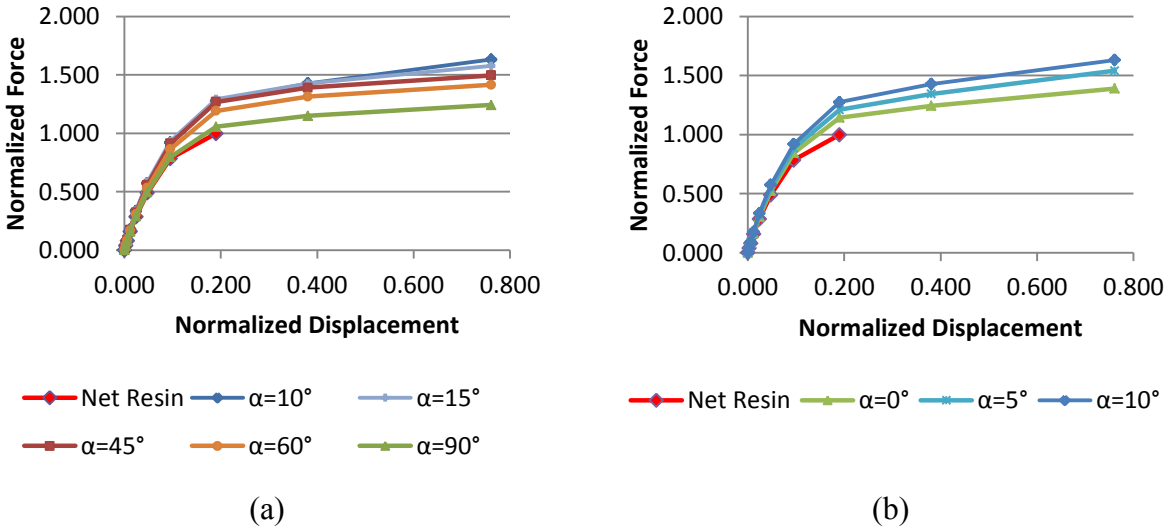

Figure 6. Resultant force (normalized by the maximal force of the unreinforced polymer) as a function of the upper block displacement (normalized by the thickness of the middle layer). (a) orientation angles above 10°. (b) orientation angles below 10°.

Excerpt from ISBN 978-3-00-053387-7

The CNT strengthens the matrix by transferring a part of the applied load from upper to lower region. We notice that the strengthening effect is higher when the CNT orientation, α, of the is around $10°$; resistance to shear is provided through the C–C covalent bonds. For angles lower than $10°$, it seems that shear is mostly resisted by van der Waals forces acting at CNT-polymer interface, which explains the drop in resistance (Figure 6.b). For higher angles of orientation, another drop in the resistance is noticed (Figure 6.a). This can be explained by the fact that the CNT is more efficient while under tension than under a pure shear, as shown in the previous calculation. An increase in the shear resistance around 20% to 60% is observed, which is important to reduce some delamination issues.

4. Conclusions

Similar to all fiber reinforced composites, the orientation of reinforcements has a great influence on the mechanical behavior. A CNT that is perpendicular to the direction of the load yields to minimal Young's modulus, close to the one of the net matrix. Generally, many materials and geometrical parameters influence the matrix stiffness tensor, which makes it important to use realistic simulations.

The matrix stiffness tensor that was calculated by FEM shows indeed a very important improvement of the longitudinal Young's modulus of the nanocomposite, with an amount of 1% weight-fraction of CNTs.

As the control of CNTs orientation is technically difficult to achieve industrially, the mechanical behavior is not optimal in the reality. But the loss of elastic stiffness due to the random dispersion of CNTs is out-balanced by the improvement of others resistance mechanisms, such as shear strength, as emphasized in the second simulation.

The FEM model used in this work allows handling CNTs of sizes that are available industrially (lengths in the range 40 - 100 nm were used in current simulations) and this is the main point.

References

[1] M. Drissi-Habti, X. Chapeleau, F. Chapalain, A. Cordelle, F. Zhao, E. Higashi, and Y. Guéguen, ‘On The Way To Smart Bi-Reinforced Composites Taking Advantage Of Recent Advances Of Nanomaterials And Nanotechnologies ...’, presented at the 15TH EUROPEAN CONFERENCE ON COMPOSITE MATERIALS, Venice, Italy, 2012.

[2] M. Drissi-Habti and F. Zhao, ‘Modelling of nano-reinforcement by carbon nanotubes in thermosetting matrices’, in *ACUN6*, Melbourne, Australie, 2012.

[3] M. Drissi-Habti, ‘Some Advances on Smart Mono and Bi-Reinforced Composites: Impact of Nanomaterials and Nanotechnologies’, in *ACUN6*, Melbourne, Australie, 2012.

[4] M. Drissi-Habti, Y. Guéguen, J. F. Feller, and X. Chapeleau, ‘Smart Composite Structures For Transportation Infrastructures and Vehicles’, in *Transport Research Arena (TRA)*, 2014.

[5] Y. EL ASSAMI and M. DRISSI-HABTI, ‘Modelling of effective mechanical properties of carbon nanotube reinforced polymer composites using finite element approach’, Submitted.

[6] R. S. Ruoff, D. Qian, and W. K. Liu, ‘Mechanical properties of carbon nanotubes: theoretical predictions and experimental measurements’, *Comptes Rendus Phys.*, vol. 4, no. 9, pp. 993–1008, Nov. 2003.

[7] M. Meo and M. Rossi, ‘Prediction of Young’s modulus of single wall carbon nanotubes by molecular-mechanics based finite element modelling’, *Compos. Sci. Technol.*, vol. 66, no. 11–12, pp. 1597–1605, Sep. 2006.

[8] K. I. Tserpes, P. Papanikos, and S. A. Tsirkas, ‘A progressive fracture model for carbon nanotubes’, *Compos. Part B Eng.*, vol. 37, no. 7–8, pp. 662–669, Oct. 2006.

[9] J. Gou and K. Lau, ‘Modeling and simulation of carbon nanotube/polymer composites’, *Chapter Handb. Theor. Comput. Nanotechnol. Am. Sci. Publ. In*, pp. 20051–58883, 2005.

Excerpt from ISBN 978-3-00-053387-7

[10] Q. H. Zeng, A. B. Yu, and G. Q. Lu, 'Multiscale modeling and simulation of polymer nanocomposites', *Prog. Polym. Sci.*, vol. 33, no. 2, pp. 191–269, Feb. 2008.

[11] S. B. Sinnott, O. A. Shenderova, C. T. White, and D. W. Brenner, 'Mechanical properties of nanotubule fibers and composites determined from theoretical calculations and simulations', *Carbon*, vol. 36, no. 1–2, pp. 1–9, 1998.

[12] G. M. Odegard, T. S. Gates, K. E. Wise, C. Park, and E. J. Siochi, 'Constitutive modeling of nanotube–reinforced polymer composites', *Compos. Sci. Technol.*, vol. 63, no. 11, pp. 1671–1687, Aug. 2003.

[13] C. Li and T.-W. Chou, 'A structural mechanics approach for the analysis of carbon nanotubes', *Int. J. Solids Struct.*, vol. 40, no. 10, pp. 2487–2499, May 2003.

[14] H. J. B. Liu, 'Atomic-scale finite element method in multiscale computation with applications to carbon nanotubes', *Phys Rev B*, vol. 72, no. 3, 2005.

[15] K. I. Tserpes and P. Papanikos, 'Finite element modeling of single-walled carbon nanotubes', *Compos. Part B Eng.*, vol. 36, no. 5, pp. 468–477, Jul. 2005.

[16] X. Lu and Z. Hu, 'Mechanical property evaluation of single-walled carbon nanotubes by finite element modeling', *Compos. Part B Eng.*, vol. 43, no. 4, pp. 1902–1913, Jun. 2012.

[17] L. Y. Jiang, Y. Huang, H. Jiang, G. Ravichandran, H. Gao, K. C. Hwang, and B. Liu, 'A cohesive law for carbon nanotube/polymer interfaces based on the van der Waals force', *J. Mech. Phys. Solids*, vol. 54, no. 11, pp. 2436–2452, Nov. 2006.

[18] X. Q. He, S. Kitipornchai, C. M. Wang, and K. M. Liew, 'Modeling of van der Waals force for infinitesimal deformation of multi-walled carbon nanotubes treated as cylindrical shells', *Int. J. Solids Struct.*, vol. 42, no. 23, pp. 6032–6047, Nov. 2005.

[19] D. Qian, E. C. Dickey, R. Andrews, and T. Rantell, 'Load transfer and deformation mechanisms in carbon nanotube-polystyrene composites', *Appl. Phys. Lett.*, vol. 76, no. 20, pp. 2868–2870, May 2000.

[20] B. Fiedler, F. H. Gojny, M. H. G. Wichmann, M. C. M. Nolte, and K. Schulte, 'Fundamental aspects of nano-reinforced composites', *Compos. Sci. Technol.*, vol. 66, no. 16, pp. 3115–3125, Dec. 2006.

[21] A. Montazeri and N. Montazeri, 'Viscoelastic and mechanical properties of multi walled carbon nanotube/epoxy composites with different nanotube content', *Mater. Des.*, vol. 32, no. 4, pp. 2301–2307, Apr. 2011.

[22] F. Vahedi, H. R. Shahverdi, M. M. Shokrieh, and M. Esmkhani, 'Effects of carbon nanotube content on the mechanical and electrical properties of epoxy-based composites', *New Carbon Mater.*, vol. 29, no. 6, pp. 419–425, Dec. 2014.

[23] D. W. Brenner, O. A. Shenderova, J. A. Harrison, S. J. Stuart, B. Ni, and S. B. Sinnott, 'A second-generation reactive empirical bond order (REBO) potential energy expression for hydrocarbons', *J. Phys. Condens. Matter*, vol. 14, no. 4, p. 783, 2002.

[24] X.-L. Gao and K. Li, 'A shear-lag model for carbon nanotube-reinforced polymer composites', *Int. J. Solids Struct.*, vol. 42, no. 5–6, pp. 1649–1667, Mar. 2005.

[25] T. Chang and H. Gao, 'Size-dependent elastic properties of a single-walled carbon nanotube via a molecular mechanics model', *J. Mech. Phys. Solids*, vol. 51, no. 6, pp. 1059–1074, Jun. 2003.

[26] C. Li and T.-W. Chou, 'Multiscale Modeling of Carbon Nanotube Reinforced Polymer Composites', *J. Nanosci. Nanotechnol.*, vol. 3, no. 5, pp. 423–30, 2003.

[27] F. Scarpa and S. Adhikari, 'A mechanical equivalence for Poisson's ratio and thickness of C–C bonds in single wall carbon nanotubes', *J. Phys. Appl. Phys.*, vol. 41, no. 8, p. 085306, 2008.

[28] H. Cease, P. Derwent, H. Diehl, J. Fast, and D. Finley, 'Measurement of mechanical properties of three epoxy adhesives at cryogenic temperatures for CCD construction', *Fermi Natl. Accel. Lab.*, 2006.

Excerpt from ISBN 978-3-00-053387-7